Chatter detection in robotic drilling operations combining multi-synchrosqueezing transform and energy entropy

Jianfeng Tao[1] · Hongwei Zeng[1] · Chengjin Qin[1] · Chengliang Liu[1]

Abstract
Robotic drilling shows higher efficiency and precision than the manual drilling, which has great application prospects in the aviation manufacturing. Nevertheless, due to the detrimental effects on surface quality, tool wear, the safety of the robot and machining efficiency, chatter vibration has been a major obstacle to achieve stable and efficient robotic drilling. Therefore, it is particularly significant to detect and manage to suppress the chatter as early as possible. This paper presents a novel approach to identify the chatter in robotic drilling process based on multi-synchrosqueezing transform (MSST) and energy entropy. To begin with, matrix notch filters are designed to effectively eliminate the interference of spindle rotating frequency and its harmonics to the measured vibration signal. Subsequently, the filtered signal is processed by the MSST to obtain concentrated time-frequency representation. Then, the signal is divided equally into finite frequency bands and the subcomponent corresponding to each frequency band is reconstructed through the reverse MSST. Finally, in consideration of the change of the vibration signal in frequency and energy distribution when chatter occurs, the energy entropy is computed as the chatter detection indicator. The proposed chatter detection method was validated by robotic drilling experiments with different tools, machining parameters, and workpiece material, and the results indicate that the proposed method can effectively detect the chatter before it is fully developed and recognize the chatter earlier than the synchroextracting-based method.

Keywords Robotic drilling process · Chatter detection · Matrix notch filter · Multi-synchrosqueezing transform · Energy entropy

1 Introduction

Over the past decade, robotic machining has gained increasingly attention because of its high flexibility and large working envelope [1, 2]. For instance, in the aviation manufacturing, industrial robots have shown great application prospects, which can efficiently accomplish drilling works of thousands of aircraft intersection holes [3]. However, the application of robotic machining is still very limited in actual production at present. Compared with the conventional machine tools, serial robot manipulators are more likely to chatter due to the lower stiffness [4, 5]. It is known that chatter brings various negative impacts on the machining process, including accelerating the

✉ Chengjin Qin
   qinchengjin@sjtu.edu.cn

1   State Key Laboratory of Mechanical System and Vibration, School of Mechanical Engineering, Shanghai Jiao Tong University, Shanghai 200240, China

tool wear, lowering the machining quality, and even affecting the safety of the robot. For these reasons, chatter has been a major obstacle to realize stable and efficient robotic drilling [6]. To avoid the detriments caused by the chatter, researches on the stability analysis, detection and suppression of such detrimental instability have become a heated topic in academia and industry [7–15].

So far, researchers have conducted in-depth researches on chatter suppression and proposed many effective suppression methods, including selection of chatter-free cutting parameters, variable spindle speed, passive chatter control, and active chatter control. Theoretically speaking, the occurrence of chatter can be prevented by adopting appropriate cutting parameters based on the stability lobe diagrams [15]. However, due to the heterogeneous stiffness of robot within its working envelope, it is difficult to guarantee the robotic drilling process without chatter by the selected fixed machining parameters [4]. Fortunately, there is a certain time interval from chatter onset to mature chatter, and accurate detection and timely suppression provide an alternative feasible approach to avoid the hazards of chatter. If chatter can be identified accurately at

an early stage, there will be enough time to implement appropriate measures to suppress its further development. Hence, accurate and timely detection of chatter is of vital significance to avoid the adverse effects of chatter on the machining system.

In order to automatically detect chatter, various chatter-related signals can be acquired, including vibration signal [16–20], torque signal [21, 22], motor current signal [23–25], and sound signal [26–28]. In industrial applications, vibration signal stands out from these signals owing to its information usability, low cost, and easy access [29], which has been widely adopted for chatter detection. Chatter vibration is a typical kind of self-excited vibration between the cutter and the workpiece. Due to the regenerative effect, the occurrence of chatter will usually cause changes in energy distribution and frequency components. However, during the early stage of chatter development, the chatter features are extremely weak. Consequently, it is necessary to choose an appropriate signal processing tool to extract the required chatter features from the signal. In the last decades, time domain analysis and spectral analysis methods have been employed to detect chatter [30, 31]. In view of the nonlinear and nonstationary properties of chatter signal, time-frequency analysis (TFA) methods that preserve both time-domain and frequency-domain information have gradually become the prior choice approaches for chatter signal analysis. So far, short-time Fourier transform (STFT), wavelet transform (WT), wavelet packet transform (WPT), and empirical mode decomposition (EMD) have been used for chatter detection [32–35]. For instance, Tangjitsitcharoen et al. [34] adopted wavelet transform to process the cutting forces signals in ball end milling process for chatter detection. In [23], WPT was utilized to monitor the energy change of motor current signal to identify chatter in gear grinding process. Liu et al. [35] investigated a milling chatter identification method, in which EMD and wavelet packet decomposition (WPD) was combined to eliminate the influence of modal aliasing. Although these methods based on the conventional TFA methods achieved certain effects, they are without exception limited by the Heisenberg uncertainty principle, which stipulates that a signal cannot be localized with an arbitrary precision both in time and frequency.

To improve the performance of classical TFA methods, researchers have proposed some advanced methods in the past few years. The reassignment method (RM) is a kind of high-resolution TFA methods which aims to sharpen the time-frequency (TF) representation while keeping the temporal localization, but it is very limited in engineering applications because it cannot reconstruct the signal [36]. To overcome these drawbacks, Daubechies et al. [37] developed the synchrosqueezing transform (SST) which can achieve high-resolution TF representation and meanwhile retain the signal reconstruction ability. After that, many improved methods have been proposed, e.g., synchroextracting transform (SET) [38], demodulated SST (DSST) [39], and high-order SST

[40]. These advanced TFA methods have been utilized for chatter detection and achieved better performance. For instance, Cao et al. [26] introduced a chatter detection approach in milling process based on SST of sound signals. Also, Tao et al. [41] employed the SET to analyze the vibration signal and realized the early chatter identification in robotic drilling process. However, the SST is very sensitive to signal noise and has poor noise robustness, while SET may suffer large reconstruction errors when processing strong nonstationary signals due to lack of perfect signal reconstruction. More recently, Yu et al. [42] proposed a novel TFA method termed multi-synchrosqueezing transform (MSST), which concentrated the energy of the TF result by iteratively employing multiple SST operations. Compared with the other methods mentioned above, MSST can obtain higher resolution TF representation when dealing with the strongly time-varying signals, and meanwhile retain excellent signal reconstruction ability. Therefore, MSST is an ideal signal processing tool for chatter detection.

During the robotic drilling process, the energy distribution and frequency components of vibration signal changes with the machining state. Under the stable machining state, rotation frequency and its harmonics are dominant. When the machining state transitions to chatter, new dominant frequency components will appear and the energy will be transferred to the chatter frequency gradually [41]. Hence, the change of energy distribution can be used to characterize chatter. To quantify the change of the system energy distribution, energy entropy is introduced as the chatter indicator. It is worth noting that chatter frequency is easy to be merged by rotation frequency and its harmonics in the early stages of chatter [43]. Therefore, it is desperately needed to eliminate the disturbance of rotational-related frequencies to the measured signal. Based on the analysis above, this paper develops a novel approach for chatter detection based on MSST and energy entropy, in which weak chatter features during early development stage can be keenly captured. The remainder of this paper is structured as follows. In the next section, the proposed chatter detection method is developed in detail. Section 3 presents the experimental verification for the proposed method, including the experimental setup, the experimental results, and the analysis. Finally, the conclusion is drawn in Sect. 4.

2 Multi-synchrosqueezing-based method

2.1 Matrix notch filter

It is well recognized that the spindle rotating frequency and its harmonics always exist throughout the machining process. In particular, during the early stage of chatter, because the forced vibration is dominant, the rotational-related frequencies still prevail while the chatter components are exceedingly weak. If

the weak chatter frequencies are submerged by the rotational-related frequencies, the chatter indicator extracted from the vibration signal may have no distinct change, resulting in a time lag in the chatter detection. Consequently, the rotational-related components should be discarded to ensure that the chatter can be recognized as early as possible.

As an effective filtering tool, notch filter is capable of rejecting just one specific frequency from the signal. It is typically adopted to eliminate the sinusoidal or narrow-band interference while keeping the broadband signal unchanged. Moreover, considering that the data used for analysis in the chatter detection belongs to the short data records, the selected method should have good filtering performance for short data. However, when processing short data records, the conventional IIR notch filters show unsatisfactory performance due to the occurrence of the transient state while the FIR notch filters have higher orders under the same requirement [44]. To achieve better transient performance when filtering short data records, the key to designing the notch filter is obtaining the transfer function with frequency response as close as possible to the ideal notch filter [45]. The specific design algorithm for the optimal matrix notch filter is described below.

Define $\mathbf{H}_{\omega_s}$ as a matrix notch filter with the notch frequency ω_s. Let $\mathbf{x} = [\mathbf{x}(0), \mathbf{x}(1),\ldots, \mathbf{x}(N-1)]^T$ be input signal to the matrix notch filter whose output is $\mathbf{y} = [\mathbf{y}(0), \mathbf{y}(1),\ldots, \mathbf{y}(N-1)]^T$. Then, the filtering operation can be expressed as $\mathbf{y} = \mathbf{H}_{\omega_s}\mathbf{x}$. Define a vector of the complex exponentials $\underline{\mathbf{v}}(\omega)$ as $\underline{\mathbf{v}}(\omega) = [1, e^{j\omega}, e^{j2\omega},\ldots, e^{j(N-1)\omega}]^T$, and the output of the ideal matrix notch filter should satisfy

$$\mathbf{H}_{\omega_s}\mathbf{v}(\omega) = \begin{cases} 0 & \omega = \omega_s \\ \mathbf{v}(\omega) & \omega \neq \omega_s \end{cases} \tag{1}$$

The passband of the notch filter is $P = [0, \omega_s-\varepsilon]\cup[\omega_s+\varepsilon, \pi]$, where ε is a small positive number. By inserting K uniformly spaced points in the passband P, one can obtain

$$\omega_i = \frac{\pi-2\varepsilon}{K}, i = 1, 2, \ldots, K \tag{2}$$

where ω_i are uniform dense grid frequency points in the passband P.

Substitute ω_i and ω_s in the vector $\mathbf{v}(\omega)$ and then split $\mathbf{v}(\omega)$ into the real part $\mathbf{v}_R(\omega)$ and the imaginary part $\mathbf{v}_I(\omega)$. Define two matrices as follows

$$V = [\mathbf{v}_R, \mathbf{v}_I] \tag{3}$$

$$W = [\mathbf{v}_R(\omega_S), \mathbf{v}_I(\omega_S)] \tag{4}$$

where $\mathbf{V}_R = [\mathbf{v}_R(\omega_1), \mathbf{v}_R(\omega_2),\ldots, \mathbf{v}_R(\omega_K)]$ and $\mathbf{V}_I = [\mathbf{v}_I(\omega_1), \mathbf{v}_I(\omega_2),\ldots, \mathbf{v}_I(\omega_K)]$.

The ideal notch filter $\mathbf{H}_{\omega_s}$ should meet the conditions $\mathbf{H}_{\omega_s}\mathbf{V} = \mathbf{V}$ and $\mathbf{H}_{\omega_s}\mathbf{W} = 0$. Let $\mathbf{h}_l$ and $\mathbf{v}_l$ denote the lth column vectors of matrices $(\mathbf{H}_{\omega_s})^T$ and $\mathbf{V}^T$, respectively. According to

the least squares method, the $\mathbf{h}_l$ is determined by minimizing the cost function

$$J = \left\| \mathbf{V}^T\mathbf{h}_l - \mathbf{h}_l \right\|^2 \tag{5}$$

whose constraint is $\mathbf{Wh}_l = 0$. This optimization problem can be solved by Lagrange multiplier method, and its closed form solution is

$$\mathbf{h}_l = \mathbf{Q}^{-1}\mathbf{V}\mathbf{v}_l - \mathbf{Q}^{-1}\mathbf{W}^T\left(\mathbf{W}\mathbf{Q}^{-1}\mathbf{W}^T\right)^{-1}\mathbf{W}\mathbf{Q}^{-1}\mathbf{v}_l \tag{6}$$

where $\mathbf{Q} = (\mathbf{V}\mathbf{V}^T)^{-1}$. Compose all column vectors $\mathbf{h}_l$ column by column and the optimal matrix notch filter can be finally written as

$$\mathbf{H}_{\omega_s} = \mathbf{I} - \mathbf{W}\left(\mathbf{W}^T\mathbf{Q}\mathbf{W}\right)^{-1}\mathbf{W}^T\mathbf{Q}^T \tag{7}$$

2.2 Multi-synchrosqueezing transform

The essence of MSST is to iteratively execute multiple SST operations. For clear description of the MSST principle, SST is reviewed briefly at first. SST is a post-processing procedure on the conventional TFA methods and it is introduced based on an STFT framework in this section. The STFT of the signal $x(t)$ is represented as

$$F_x(\tau, \omega) = \int_{-\infty}^{\infty} x(t)g(t-\tau)e^{-j\omega(t-\tau)}dt \tag{8}$$

where $g(t)$ is the compactly supported window function. The regular definition of STFT differs from Eq. (8) by a phase shift factor $e^{j\omega t}$. Define $x(t)$ as a mono-component signal, i.e., $x(t) = A(t)e^{-j\phi(t)}$. According to Parseval's theorem, the STFT of $x(t)$ is given by

$$F_x(\tau, \omega) = A(t)\cdot\hat{g}(\omega-\phi'(\tau))\cdot e^{j\phi(\tau)} \tag{9}$$

where $\hat{g}(\omega-\phi'(\tau))$ denotes the Fourier transform of the window function. If $F_x(\tau, \omega) \neq 0$, the instantaneous frequency estimate $\varpi(\tau, \omega)$ for the STFT result can be approximated by

$$\widetilde{\omega}(\tau, \omega) = -j\frac{\partial_t F_x(\tau, \omega)}{F_x(\tau, \omega)} \tag{10}$$

where $\partial_t F_x(\tau, \omega)$ means the partial derivative of the variable t, namely, $\partial_t F_x(\tau, \omega) = \partial F_x(\tau, \omega)/\partial t$.

The SST employs a frequency reallocation operator to gather all FT coefficients with the same instantaneous frequency, which is expressed as

$$TF(\tau, \psi) = \int_{-\infty}^{+\infty} F_x(\tau, \omega)\cdot\delta(\psi-\widetilde{\omega}(\tau, \omega))d\omega \tag{11}$$

where δ denotes the Dirac function.

The basic idea of MSST is to repeatedly apply another SST operation to the already acquired SST result to obtain a much

sharper TF result than previous result. Through multiple iterations of SST, the energy of the TF representation can be concentrated in a step-wise manner. Assuming that the iteration times is N ($N \geq 2$), MSST can be formulated as

$$TF^{[2]}(\tau, \psi) = \int_{-\infty}^{+\infty} TF^{[1]}(\tau, \omega) \cdot \delta(\psi - \widetilde{\omega}(\tau, \omega)) \, d\omega \quad (12)$$

$$TF^{[3]}(\tau, \psi) = \int_{-\infty}^{+\infty} TF^{[2]}(\tau, \omega) \cdot \delta(\psi - \widetilde{\omega}(\tau, \omega)) d\omega$$

$$\vdots$$

$$TF^{[N]}(\tau, \psi) = \int_{-\infty}^{+\infty} TF^{[N-1]}(\tau, \omega) \cdot \delta(\psi - \widetilde{\omega}(\tau, \omega)) d\omega$$

where $TF(\tau, \psi)$ in Eq. (11) is denoted by $TF [1](\tau, \omega)$. Combining Eq. (11) and Eq. (12), the formula of the MSST can be rewritten as

$$TF^{[N]}(\tau, \psi) = \int_{-\infty}^{+\infty} F_x(\tau, \omega) \cdot \delta\left(\psi - \varpi^{[N]}(\tau, \omega)\right) d\omega \quad (13)$$

where $\widetilde{\omega}^{[N]}(\tau, \omega)$ denotes the instantaneous frequency estimate of MSST. It can be obtained by a recursive algorithm, namely

$$\widetilde{\omega}^{[N]}(\tau, \omega) = \underbrace{\widetilde{\omega}(\tau, \widetilde{\omega}(\tau, \widetilde{\omega}(\tau, \widetilde{\omega}(\tau, \cdots \widetilde{\omega}(\tau, \omega) \cdots)))))}_{N}$$

$$(14)$$

in which $\varpi(\tau, \omega)$ can be calculated by Eq. (10).

MSST allows for the perfect signal reconstruction. Let ψ_k and ψ_{k+1} be the lower and upper limits of the kth frequency band, and then the subsignal corresponding to the frequency band can be recovered as follows

$$x_k(t) = \frac{1}{2\pi g(0)} \int_{\psi_k}^{\psi_{k+1}} TF^{[N]}(t, \psi) d\psi \quad (15)$$

2.3 The proposed detection algorithm

Chatter is a kind of self-excited vibration phenomenon generated by the robot when it absorbs the energy from periodic cutting forces during the drilling process. At the beginning of the chatter, chatter components are not sufficiently obvious and have the smaller amplitude than the rotational-related frequency. Consequently, in order to identify the chatter effectively, it is necessary to obtain the high-resolution TF representation and seek a sensitive indicator that can accurately reflect the energy distribution change of the measured signal. Meanwhile, the rotational-related components need to be removed to prevent them from submerging the chatter frequency before the chatter characteristic extraction.

On the basis of discussion above, a novel chatter detection approach based on MSST and energy entropy is proposed in this paper. The flowchart of the proposed scheme is illustrated in Fig. 1. As the basic work, the
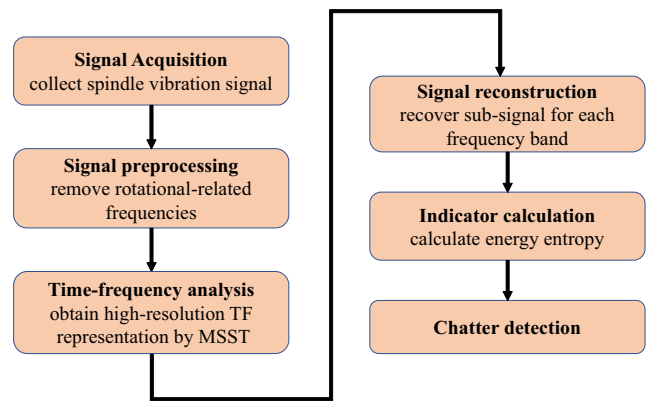

Fig. 1 The flowchart of the proposed algorithm for chatter detection

accelerometer is first installed to measure the vibration signals during the robotic drilling process. Based on the measured vibration signals, the chatter identification algorithm is developed and it is implemented in four steps. Firstly, the rotational-related frequencies are filtered out from the measured vibration signal by using the designed optimal matrix notch filters. Secondly, the MSST is utilized to address the filtered signal and acquire the concentrated TF representation. Then, the entire TF representation is divided into several equally spaced frequency bands and the reconstruction operation is performed to generate the subsignal in each frequency band. At last, the energy entropy of the whole signal is calculated in time for chatter detection.

Specifically, in the first step of the proposed algorithm, matrix notch filters are designed to remove the rotation frequency and its harmonics. Suppose $\omega_{s1}, \omega_{s2}, \ldots, \omega_{sk}$ represent spindle rotating frequency and its harmonics, and $\mathbf{H}_{\omega_{s1}}, \mathbf{H}_{\omega_{s2}}, \ldots, \mathbf{H}_{\omega_{sk}}$ are the corresponding optimal matrix notch filters. Given the measured vibration signal $\mathbf{s}_i = [\mathbf{s}_i(1), \mathbf{s}_i(2), \ldots, \mathbf{s}_i(L)]^T$, the filtered output signal $\mathbf{s}_o = [\mathbf{s}_o(1), \mathbf{s}_o(2), \ldots, \mathbf{s}_o(L)]^T$ can be obtained as

$$\mathbf{s}_o = \mathbf{H}\mathbf{s}_i = (\mathbf{H}_{\omega_{sk}} \cdots \mathbf{H}_{\omega_{s2}} \cdot \mathbf{H}_{\omega_{s1}})\mathbf{s}_i \quad (16)$$

where $\mathbf{H}_{\omega_{s1}}, \mathbf{H}_{\omega_{s2}}, \ldots, \mathbf{H}_{\omega_{sk}}$ can be calculated by Eq. (7). To obtain the energy-concentrated TF results, the filtered signal $\mathbf{s}_o$ is analyzed by the MSST, which can reconstruct the signal perfectly. Considering that $\mathbf{s}_o$ is discrete, the discrete STFT is presented as

$$F_x[d, m] = \sum_{l=1}^{L} \mathbf{s}_o[l] g[l-d] e^{-j\frac{2\pi}{L}m[l-d]} \quad (17)$$

According to Eq. (10), the discrete form of instantaneous frequency estimate $\hat{\omega}[d, m]$ can be deduced as

$$\hat{\omega}[d, m] \begin{cases} \text{Ro}\left[\text{Re}\left[\frac{1}{2\pi j}\ln\left[\frac{F_x[d+1,m]}{F_x[d,m]}\right]\right]\right] & , F_x[d,m] \neq 0 \\ 0 & , F_x[d,m] = 0 \end{cases} \quad (18)$$

where Re[] denotes taking real part. And Ro[] represents the round operation, which rounds the variable to the nearest integer. For instance, Ro[3.1] = 3 and Ro[3.8] = 4.

Then, according to Eq. (13), the TF distribution of $\mathbf{s}_o$ can be written as

$$TF^{[N]}[d, \eta] = \sum_{m=1}^{L} F_x[d, m]\delta\left[\eta - \hat{\omega}^{[N]}[d, m]\right] \quad (19)$$

where $\hat{\omega}^{[N]}[d, m]$ can be obtained by combining Eq. (14) and Eq. (18).

In theory, the chatter can be identified by observing whether there are significant chatter frequencies in the obtained high-resolution TF representation. However, this method cannot achieve the automatic chatter detection and it is difficult to identify the chatter at the early stage. Thus, the energy entropy is chosen as the chatter indicator to depict the energy distribution changes of the vibration signal. To calculate the energy entropy of the signal, it is necessary to divide the whole signal $s(t)$ into a finite number of frequency bands and recover the subsignals corresponding to each frequency band. Let $\Delta\eta$ be the bandwidth of each frequency band. According to the reconstruction formula Eq. (15), the corresponding subsignal can be expressed as

$$S_k[d] \approx \frac{1}{2\pi g(0)} \sum_{\eta \in [\eta_k, \eta_k + \Delta\eta]} TF^{[N]}[d, \eta] \quad (20)$$

For each reconstructed subsignal, their energy is calculated as

$$E_k = \sum_{j=1} s_k\left[d_j\right]^2, \quad k = 1, 2, \cdots, n \quad (21)$$

Finally, the energy entropy MSSTE of the whole signal can be acquired as

$$MSSTE = \sum_{k=1}^{n} E_k \ln(E_k) \quad (22)$$

The energy entropy MSSTE is an indicator with good performance, which is quite sensitive to the chatter. With the occurrence of chatter, the energy of the system is transferred to the frequency band where chatter frequency is located, and the energy entropy MSSTE will dramatically increase. Accordingly, during the robotic drilling process, timely chatter detection can be perfectly performed by calculating the energy entropy of the vibration signal and comparing it with the chatter threshold in real time. If the energy entropy exceeds the threshold, it is indicated that chatter is detected and appropriate vibration suppression measures should be taken. If not, the robotic drilling process is stable. It can be seen that the chatter threshold plays a critical role in the proposed algorithm. In consideration of the versatility and effectiveness, the chatter threshold should be determined on the basis of numerous robotic drilling experiments.

3 Verification and comparisons

3.1 Experimental setup

In order to verify the actual effect of the proposed algorithm, a series of drilling experiments with different cutting conditions were carried out on a robot drilling machining experimental platform, as shown in Fig. 2. The platform consists mainly of a KUKA industrial robot, a drilling end actuator, the workpiece and the corresponding fixture, sensors and a data acquisition system. The drilling end actuator is mounted on the end of the robot through flanges, which is composed of a spindle module, a feed module, a visual measurement module, a normal detection module, and a pressure foot. The spindle module and the feed module are used to realize the drilling operation, and the visual measurement module provides the precise positioning of the reference hole. The strict verticality of the drilling hole is ensured through the normal detection module, by which the normal line of the workpiece can be measured accurately. To improve the stiffness of the system, a relatively large pressing force is applied to the workpiece by the pressure foot during the robotic drilling process.

To measure the vibration signals of the spindle of the robotic drilling process, we selected the PCB 356A24 accelerometer and attached it to the nonrotating part of the spindle closest to the tool with adhesive, as shown in Fig. 3. It is a triaxial, ceramic shear accelerometer and has a voltage output. The frequency range of PCB 356A24 is from 0.5 to 12,000 Hz, and the sensitivity of the X-, Y-, and Z-axes is 1.043 mv/m/s^2, 1.035 mv/m/s^2, and 1.064 mv/m/s^2, respectively. Since the vibration signal of the X-axis is more sensitive to chatter than that of the Y-axis and the Z-axis (parallel to the feed direction), it is used for chatter detection. Taking the high-frequency properties of chatter components into account, the data acquisition system (the Crystal Instruments CoCo-80) collected acceleration signals at a sampling frequency of 10,240 Hz. Two
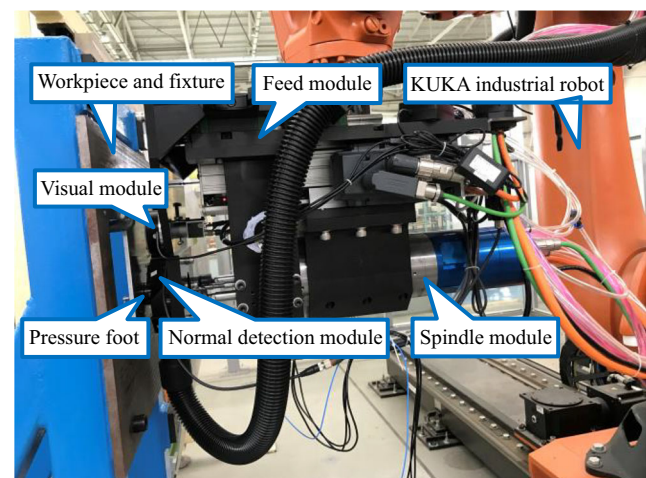

Fig. 2 The experimental platform for robotic drilling machining
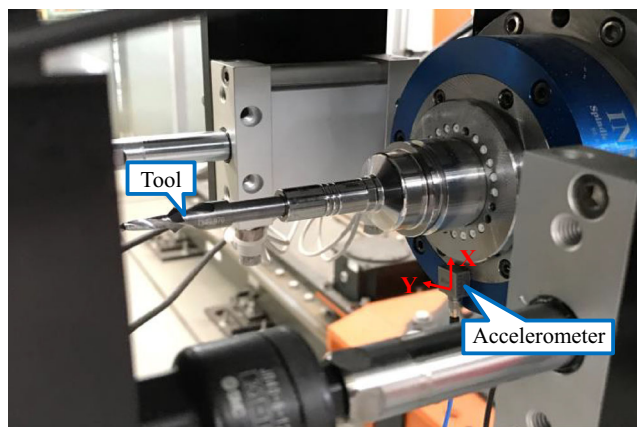
Fig. 3 Illustration of accelerometer installation

different uncoated hard alloy steel drilling-countersinking tools with different geometrical shapes were used. Specifically, the tool A has a diameter of 5 mm, 130° point angle, and 100° countersink angle, while the tool B is characterized by the 6 mm diameter, 120° point angle, and 100° countersink angle.

3.2 Results and comparisons

Robotic drilling experiments under different cutting parameters were performed to validate the proposed method. Two kinds of aerospace aluminum alloy workpiece, i.e., AL7075 and AL606, were used in the experiments. To avoid accidental factors affecting the results, all the experiments with the same machining parameters were repeated three times. The drilling mode was dry drilling without lubricants and coolants. To better observe the surface quality of holes, the drilling holes were all blind holes. Notice that whether chatter occurs during robotic drilling process is evaluated by combining the surface quality of the drilling holes, the amplitude, and the spectrum of the acceleration signal. The surface quality of chattered hole and normal hole is illustrated in Fig. 4. It is clearly seen that chatter left obvious vibration marks on the surface of the hole, while the normal hole has smooth surface.

During the robotic drilling process, the proposed chatter detection algorithm is carried out every 25 ms. Time length

of the sample signal for a calculation is 50 ms, which corresponds to 512 sample data at the sampling frequency of 10,240 Hz. The calculated energy entropy is compared with the threshold to determine whether chatter occurs. Once the energy entropy value exceeds the threshold, it means that chatter starts. The energy entropy at different time points constitutes the trend map of the energy entropy change. At the same time, to verify the effectiveness and superiority of the proposed method, comparisons with the synchroextracting-based method in [41] is conducted. It should be noted that all calculations were done with MATLAB and no library was involved.

The first group of robotic drilling experiments were conducted with tool A. The workpiece material is aluminum alloy AL7075. Figure 5 illustrates the experimental results at spindle speed 3000 rpm and feed rate 3.0 mm/s. The energy entropy change of vibration signal in the whole drilling process is shown in Fig. 5b. At the beginning, the energy entropy is relatively small and remains unchanged basically, which corresponds to the stable robotic drilling stage. It can also be demonstrated from Fig. 5a, where the amplitude of vibration is small during the corresponding period. After $t = 0.198$ s, the energy entropy begins to increase gradually and exceeds the preset threshold at the moment $t1 = 0.470$ s, which means that the chatter is detected by the proposed method. Then, the energy entropy continues to increase for a short time, but the growth rate slows down gradually. Eventually, the energy entropy stabilizes at a higher value. It can be found that the energy entropy increases dramatically and eventually far exceeds the initial value when the machining state transitions from stable to unstable. Therefore, the energy entropy can effectively characterize the machining state of the robotic drilling and is quite sensitive to the appearance of chatter. According to Fig. 5c, the relatively distinct chatter frequency emerges in the spectrogram of the MSST at about the moment $t = 0.593$ s. At the same time, the synchroextracting-based method detects chatter at the moment $t2 = 0.554$ s, which is 84 ms latter than the proposed method. As a consequence, the results demonstrate that the presented algorithm can effectively detect the chatter at an early stage during the robotic drilling process.

Fig. 4 The surface quality of chattered hole and normal hole. **a** Chatter occurs. **b** Without chatter
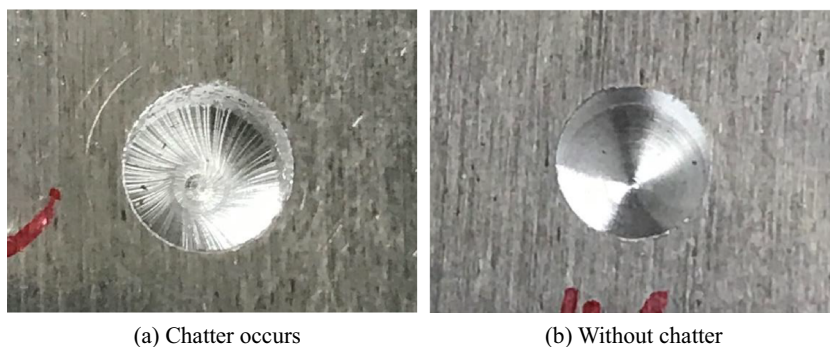
(a) Chatter occurs

(b) Without chatter

Fig. 5 Chatter test with tool A at spindle speed 3000 rpm, feed rate 3.0 mm/s. Workpiece material AL7075. **a** The vibration signal. **b** The energy entropy. **c** Time-frequency spectrum of MSST
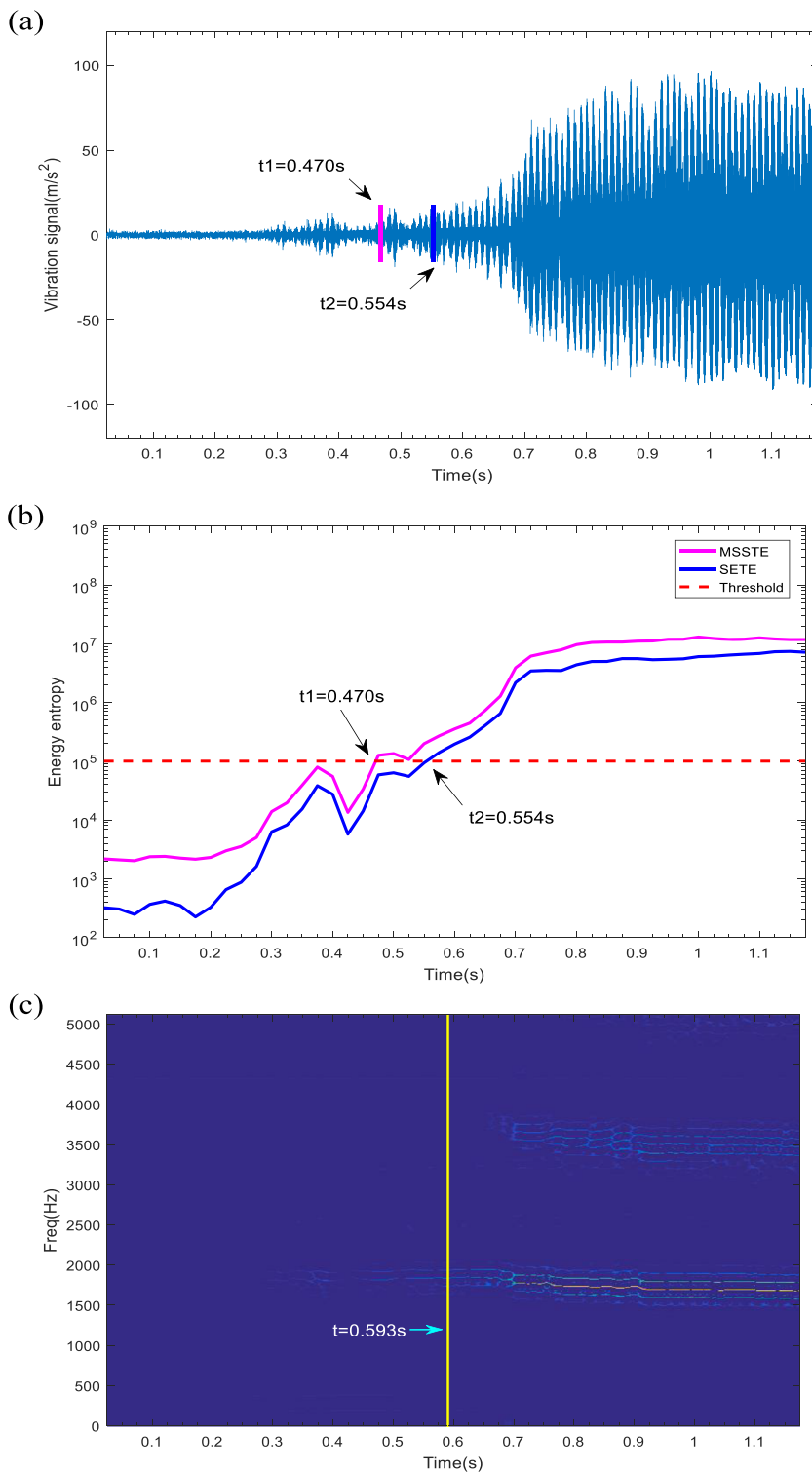
(a)

(b)

(c)

Figure 6 shows the chatter detection results for the vibration signal and the corresponding MSST spectrogram at spindle speed 4500 rpm and feed rate 3.2 mm/s. The workpiece material is also aluminum alloy AL7075. The trend map of the energy entropy change, e.g., Fig. 6b, illustrates that the energy entropy remains at a relatively low range and has a trend of slight decline before $t = 0.108$ s. As can be seen from Fig. 6a, the amplitude of the vibration is also small and relatively steady during the corresponding period, demonstrating that the robotic drilling process is stable at this moment. After $t = 0.145$ s, the energy entropy begins to rise and the rate of increase

Fig. 6 Chatter test with tool A at spindle speed 4500 rpm, feed rate 3.2 mm/s. Workpiece material AL7075. **a** The vibration signal. **b** The energy entropy. **c** Time-frequency spectrum of MSST

(a)

(b)

(c)
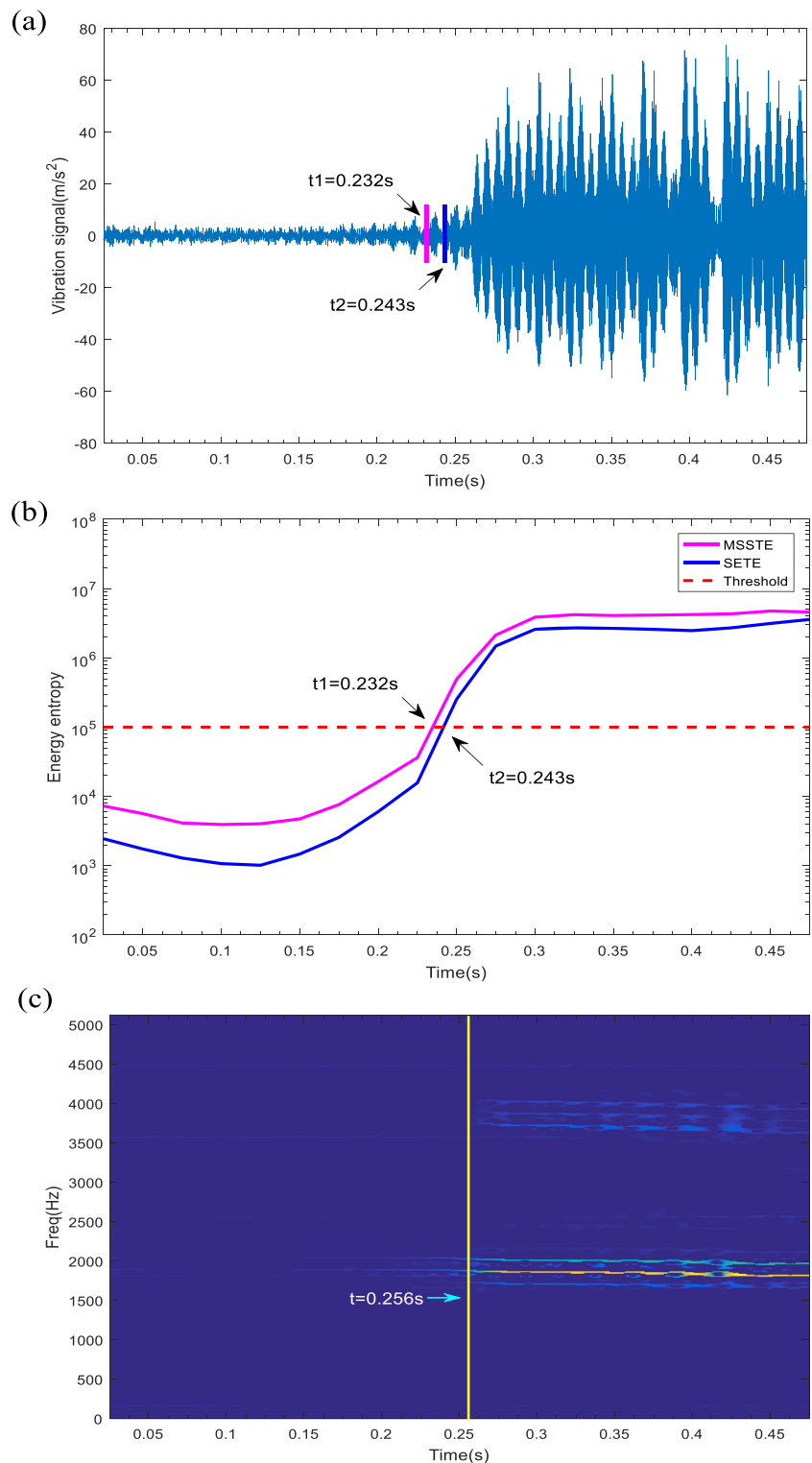
becomes faster. Then, the chatter is detected around $t1 = 0.232$ s by the proposed method and $t2 = 0.243$ s by the synchroextracting-based method. After a short period of rapid growth, the energy entropy begins to level off, indicating that the chatter has become mature. It verifies that the energy entropy can keenly depict the development of chatter. Meanwhile, according to Fig. 6c, it is at about the moment $t = 0.256$ s that the chatter frequency can be observed relatively clearly from the time-frequency spectrum of MSST. Consequently, the result verifies the effectiveness and superiority of the presented chatter detection method for robotic drilling operations.

Fig. 7 Chatter test with tool B at
spindle speed 3000 rpm, feed rate
3.5 mm/s. Workpiece material
AL6061. **a** The vibration signal. **b**
The energy entropy. **c** Time-
frequency spectrum of MSST
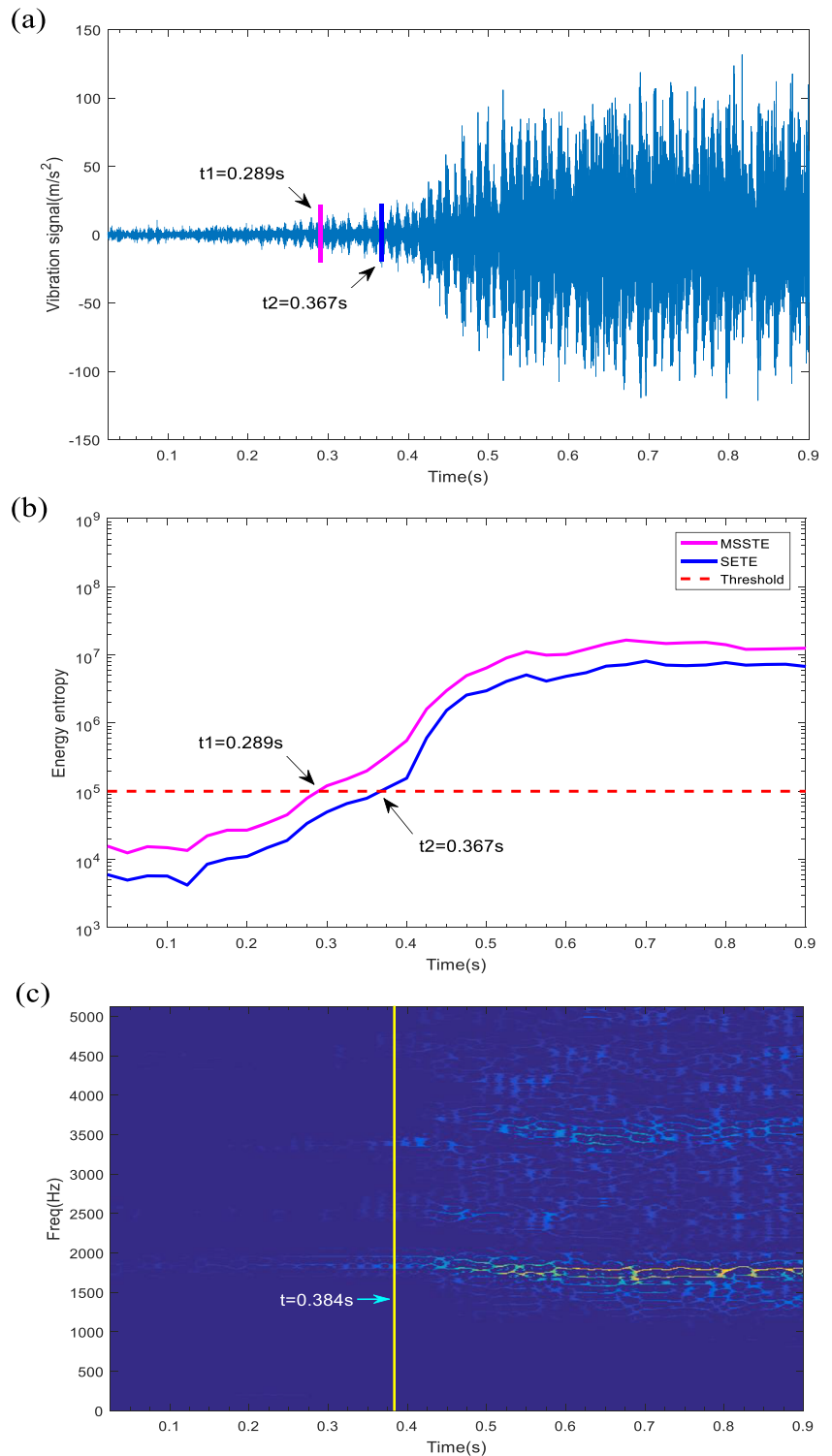
Moreover, the effectiveness and universality of the pro-
posed algorithm are further testified by more experiments with
tool B and aluminum alloy 6061 under different cutting con-
ditions. Figure 7 illustrates the chatter detection results with
spindle speed 3000 rpm and feed rate 3.5 mm/s. As shown in
Fig. 7b, the energy entropy stays at a low level and has a very

slight fluctuation in the initial stage, and it increases rapidly
after $t = 0.125$ s. It is at the moment $t1 = 0.289$ s that the chatter
is identified by the proposed method. In contrast, the
synchroextracting-based method detects chatter at the moment
$t2 = 0.367$ s. It demonstrates that the proposed method
achieves a better performance than the synchroextracting-

Fig. 8 Chatter test with tool B at
spindle speed 3000 rpm, feed rate
4.5 mm/s. Workpiece material
AL6061. **a** The vibration signal. **b**
The energy entropy. **c** Time-
frequency spectrum of MSST
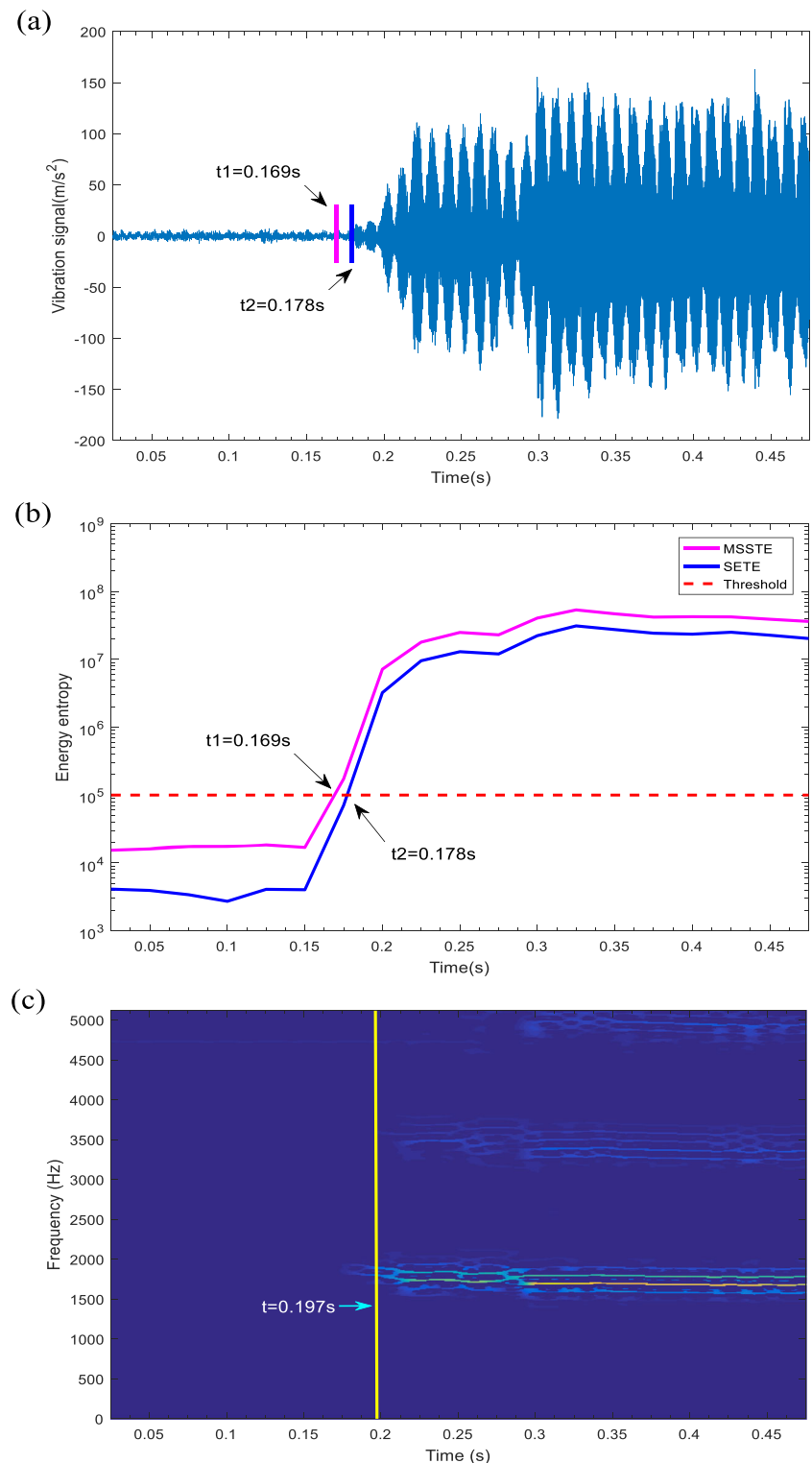
based method. Subsequently, the energy entropy gradually grows to a higher stable value, which indicates that the chatter has been fully developed. According to Fig. 7a, the amplitude of the measured vibration signal has the similar change tendency, which validates that the energy entropy can fully reflect the development process of chatter. Figure 7 c presents the time-frequency spectrum of the vibration signal acquired by MSST, where the relatively obvious chatter frequency can be observed at approximately $t = 0.384$ s. Even though the occurrence of the chatter can be detected from the Fig. 7c, it is difficult to identify the chatter at the early stage. By comparison, the proposed method can detect the chatter earlier.

The chatter detection results with spindle speed 3000 rpm and feed rate 4.5 mm/s are presented in Fig. 8. The workpiece material is aluminum alloy AL6061 as well. During the initial stage, the energy entropy almost stays constant, as shown in Fig. 8b. However, a considerable increase occurs after $t = 0.151$ s and shortly after the energy entropy exceeds the threshold value. Specifically, the chatter is detected around $t1 = 0.169$ s by the proposed method and $t2 = 0.178$ s by the synchroextracting-based method. It validates that the proposed algorithm can detect chatter earlier than the synchroextracting-based method. After that, the energy entropy continues to rise and reaches a higher stable value. As shown in Fig. 8a, there is a same trend in the amplitude of the vibration signal, but it does not increase significantly until approximately $t = 0.197$ s. It is seen that the energy entropy is very sensitive to the chatter development. It can been seen from Fig. 8c that the fundamental chatter frequency was about 1673 Hz and its second and third harmonics (3347 Hz and 5030 Hz) also appeared when chatter occurred. Actually, other experiments also had similar results, as shown in Figs. 5c, 6c, and 7c. Figure 8 c suggests that the chatter frequency becomes relatively apparent at about $t = 0.197$ s in the time-frequency spectrum. In conclusion, the result shows that the proposed method has a good performance for chatter detection and is applicable for different drilling conditions.

4 Conclusion

In this study, we develop a chatter detection method combining MSST and energy entropy for the robotic drilling process, in which weak chatter features in the early stage can be captured accurately. The spindle vibration signals are measured for chatter detection by accelerometer. In view of the principle that the chatter should be identified as early as possible, optimal matrix notch filters with good computational efficiency are designed to eliminate spindle rotating frequency and its harmonics from the measured vibration signals so as to highlight the early weak chatter components. In addition, to ensure the accuracy of chatter recognition, the MSST is adopted to analyze the filtered signals and generate a high-resolution TF representation. Then, the high-resolution TF plane is divided equally into several frequency bands and the corresponding subsignal can be recovered accurately by utilizing perfect signal reconstruction ability of MSST. Since the development of chatter is always accompanied by the change of frequency and energy distribution in vibration signal, the energy entropy of the whole signal is calculated to indicate the chatter, which has remarkable sensitivity to chatter. Robotic drilling experiments and comparisons with the synchroextracting-based method have been conducted to verify the proposed algorithm, and the results demonstrate that the proposed method can detect the weak chatter at an early stage with high effectiveness and is suitable for

different drilling conditions. In the future work, more efforts will be devoted to the construction of online chatter suppression system for robotic drilling, and the research of chatter suppression method based on sinusoidal spindle speed variation.

References

1. Iglesias I, Sebastián MA, Ares JE (2015) Overview of the state of robotic machining: current situation and future potential. Procedia Engineering 132:911–917
2. Chen Y, Dong F (2013) Robot machining: recent development and future research issues. Int J Adv Manuf Technol 66(9-12):1489–1497
3. Olsson T, Haage M, Kihlman H, Johansson R, Nilsson K, Robertsson A, Bjorkman M, Isaksson R, Ossbahr G, Brogardh T (2010) Cost-efficient drilling using industrial robots with high-bandwidth force feedback. Robot Comput Integr Manuf 26(1):24–38
4. Bu Y, Liao W, Tian W, Zhang J, Zhang L (2017) Stiffness analysis and optimization in robotic drilling application. Precision Engineering 49:388–400
5. Garnier S, Subrin K, Waiyagan K (2017) Modelling of robotic drilling. Procedia CIRP 58:416–421
6. Pan Z, Zhang H, Zhu Z, Wang J (2006) Chatter analysis of robotic machining process. J Mater Process Technol 173:301–309
7. Yuan L, Pan Z, Ding D, Sun S, Li W (2018) A review on chatter in robotic machining process regarding both regenerative and mode coupling mechanism. IEEE-ASME T Mech 23(5):2240–2251
8. Qin CJ, Tao JF, Liu CL (2017) Stability analysis for milling operations using an Adams-Simpson-based method. Int J Adv Manuf Technol 92(1–4):969–979
9. Mejri S, Gagnol V, Le T-P, Sabourin L, Ray R, Paultre P (2016) Dynamic characterization of machining robot and stability analysis. Int J Adv Manuf Technol 82(1–4):351–359
10. Qin CJ, Tao JF, Liu CL (2018) A predictor-corrector-based holistic-discretization method for accurate and efficient milling stability analysis. Int J Adv Manuf Technol 96(5–8):2043–2054
11. Safi SM, Amirabadi H, Lirabi I, Khalili K, Rahnama S (2013) A new approach for chatter prediction in robotic milling based on signal processing in time domain. Applied Mechanics and Materials 346:45–51
12. Qin CJ, Tao JF, Li L, Liu CL (2017) An Adams-Moulton-based method for stability prediction of milling processes. Int J Adv Manuf Technol 89(9–12):3049–3058
13. Guo Y, Dong H, Wang G et al (2016) Vibration analysis and suppression in robotic boring process. Int J Mach Tools Manuf 101:102–110
14. Qin CJ, Tao JF, Liu CL (2019) A novel stability prediction method for milling operations using the holistic-interpolation scheme. Proceedings of the Institution of Mechanical Engineers, Part C: Journal of Mechanical Engineering Science 233(13):4463–4475
15. Quintana G, Stepan CJ (2011) Chatter in machining processes: a review. Int J Mach Tools Manuf 51(5):363–376
16. Sun YX, Xiong ZH (2016) An optimal weighted wavelet packet entropy method with application to real-time chatter detection. IEEE/ASME Trans Mechatron 21(4):2004–2014
17. Ji Y, Wang X, Liu Z, Yan Z, Jiao L, Wang D et al (2017) EEMD-based online milling chatter detection by fractal dimension and

power spectral entropy. Int J Adv Manuf Technol 92(1-4):1185–1200

18. Chen Y, Li H, Hou L, Wang J, Bu X (2018) An intelligent chatter detection method based on EEMD and feature selection with multi-channel vibration signals. Measurement 127:356–365

19. Tao JF, Qin CJ, Xiao DY, Shi HT, Liu CL (2019) A pre-generated matrix-based method for real-time robotic drilling chatter monitoring. Chinese Journal of Aeronautics, https://doi.org/10.1016/j.cja.2019.09.001

20. Cao H, Zhou K, Chen X, Zhang X (2017) Early chatter detection in end milling based on multi-feature fusion and 3σ criterion. Int J Adv Manuf Technol 92(9-12):4387–4397

21. Tansel IN, Li M, Demetgul M, Bickraj K, Kaya B, Ozcelik B (2012) Detecting chatter and estimating wear from the torque of end milling signals by using Index Based Reasoner (IBR). Int J Adv Manuf Technol 58(1–4):109–118

22. Liu Y, Wu B, Ma J, Zhang D (2017) Chatter identification of the milling process considering dynamics of the thin-walled workpiece. Int J Adv Manuf Technol 89(5–8):1765–1773

23. Liu Y, Wang XF, Lin J, Zhao W (2016) Early chatter detection in gear grinding process using servo feed motor current. Int J Adv Manuf Technol 83(9–12):1801–1810

24. Aslan D, Altintas Y (2018) On-line chatter detection in milling using drive motor current commands extracted from CNC. Int J Mach Tools Manuf 132:64–80

25. Li Y, Zhou S, Lin J, Wang X (2016) Regenerative chatter identification in grinding using instantaneous nonlinearity indicator of servomotor current signal. Int J Adv Manuf Technol 89:799–790

26. Cao H, Yue Y, Chen X, Zhang X (2017) Chatter detection in milling process based on synchro squeezing transform of sound signals. Int J Adv Manuf Technol 89(9–12):2747–2755

27. Nair U, Krishna BM, Namboothiri VNN, Nampoori VPN (2010) Permutation entropy based real-time chatter detection using audio signal in turning process. Int J Adv Manuf Technol 46(1):61–68

28. Thaler T, Potočnik P, Bric I, Govekar E (2014) Chatter detection in band sawing based on discriminant analysis of sound features. Appl Acoust 77:114–121

29. Tao JF, Qin CJ, Xiao DY, Shi HT, Ling X, Li BC, Liu CL (2019) Timely chatter identification for robotic drilling using a local maximum synchrosqueezing-based method. J Int Manufacturing https://doi.org/10.1007/s10845-019-01509-5

30. Rafal R, Pawel L, Krzysztof K, Bogdan K, Jerzy W (2015) Chatter identification methods on the basis of time series measured during titanium superalloy milling. Int J Mech Sci 99:196–207

31. Shao Y, Deng X, Yuan Y, Mechefske CK, Chen Z (2014) Characteristic recognition of chatter mark vibration in a rolling mill based on the non-dimensional parameters of the vibration signal. J Mech Sci Technol 28(6):2075–2080

32. Liu C, Zhu L, Ni C (2018) Chatter detection in milling process based on VMD and energy entropy. Mech Syst Signal Process 105:169–182

33. Cao H, Zhou K, Chen X (2015) Chatter identification in end milling process based on EEMD and nonlinear dimensionless indicators. Int J Mach Tools Manuf 92:52–59

34. Tangjitsitcharoen S, Saksri T, Ratanakuakangwan S (2013) Advance in chatter detection in ball end milling process by utilizing wavelet transform. J Intell Manuf 26(3):1–15

35. Liu C, Zhu L, Ni C (2017) The chatter identification in end milling based on combining EMD and WPD. Int J Adv Manuf Technol 91(9-12):3339–3348

36. Auger F, Flandrin P, Lin YT, McLaughlin S, Meignen S, Oberlin T, Wu HT (2013) Time-frequency reassignment and synchrosqueezing: an overview. IEEE Signal Processing Magazine 30(6):32–41

37. Daubechies I, Lu J, H-T W (2011) Synchrosqueezed wavelet transforms: an empirical mode decomposition-like tool. Appl Comput Harmon Anal 30(2):243–261

38. Yu G, Yu M, Xu C (2017) Synchroextracting transform. IEEE Trans Ind Electron 64(10):8042–8054

39. Wang S, Chen X, Cai G, Chen B, Li X, He Z (2014) Matching demodulation transform and synchrosqueezing in time-frequency analysis. IEEE Trans Signal Process 62(1):69–84

40. Oberlin T, Meignen S, Perrier V (2015) Second-order synchrosqueezing transform or invertible reassignment? towards ideal time-frequency representations. IEEE Transactions on Signal Processing 63(5):1335–1344

41. Tao JF, Qin CJ, Liu CL (2019) A synchroextracting-based method for early chatter identification of robotic drilling process. Int J Adv Manuf Technol 100:273–285

42. Yu G, Wang ZH, Zhao P (2018) Multi-synchrosqueezing Transform. IEEE Transactions on Industrial Electronics 66(7): 5441–5455

43. Wan SK, Li XH, Chen W, Hong J (2017) Investigation on milling chatter identification at early stage with variance ratio and Hilbert–Huang transform. Int J Adv Manuf Technol 95:3563–3573

44. Piskorowski J (2010) Digital q-varying notch IIR filter with transient suppression. IEEE Trans Instrum Meas 59(4):866–872

45. Vishnu P, Ramalingam CS (2017) On the connection between matrix notch filter and maximum likelihood estimation of sinusoidal parameters. 2017 11th International Conference on Signal Processing and Communication Systems (ICSPCS), https://doi.org/10.1109/ICSPCS.2017.8270467